University of Texas Rio Grande Valley

ScholarWorks @ UTRGV

Mathematical and Statistical Sciences Faculty Publications and Presentations

College of Sciences

6-2013

Hydro-thermal convective solutions for an aquifer system heated from below

Dambaru Bhatta
The University of Texas Rio Grande Valley

Follow this and additional works at: https://scholarworks.utrgv.edu/mss_fac

 Part of the Mathematics Commons

Recommended Citation

Bhatta, D. (2013). Hydro-thermal convective solutions for an aquifer system heated from below. Applications and Applied Mathematics: An International Journal, 8(1), 15.

This Article is brought to you for free and open access by the College of Sciences at ScholarWorks @ UTRGV. It has been accepted for inclusion in Mathematical and Statistical Sciences Faculty Publications and Presentations by an authorized administrator of ScholarWorks @ UTRGV. For more information, please contact justin.white@utrgv.edu, william.flores01@utrgv.edu.

Available at
http://pvamu.edu/aam
Appl. Appl. Math.
ISSN: 1932-9466
Vol. 8, Issue 1 (June 2013), pp. 1 – 15

Applications and Applied Mathematics:
An International Journal
(AAM)

Hydro-thermal convective solutions for an aquifer system heated from below

Dambaru Bhatta

Department of Mathematics
The University of Texas-Pan American
Edinburg, Texas 78539-2999 USA
bhattad@utpa.edu

Received: January 23, 2013; Accepted: April 11, 2013

Abstract

We investigate the effect of hydro-thermal convection in an aquifer system. It is assumed that the aquifer is bounded below and above by impermeable boundaries and it is heated from below. The solution of the governing system is expressed in terms of the basic steady state solution and perturbed solution. We obtain the critical Rayleigh number and critical wavenumber using Runge-Kutta method in combination of shooting method and present the marginal stability curve. The amplitude equation is derived by introducing the adjoint system. After amplitude is obtained, we compute the linear solutions for super-critical and sub-critical cases. Numerical results for various spatial and time values are presented in graphical forms.

Keywords: convective flow; aquifer; porous media; marginal stability; adjoint

MSC 2010 No.: 35Q35; 35Q79; 76E06; 76S05

1. Introduction

A porous media consists of a solid matrix with an interconnected void. The interconnectedness of the void, the pores, allows flow of fluids through the material. Beach sand, sandstone, limestone, wood and human lung are examples of natural porous media. In a natural porous media the

distribution of pores with respect to shape and size is not regular. But in typical experiments the quantities of interest are measured over areas that cross many pores and such space averaged quantities change in a regular way and hence are amenable to theoretical treatment [Nield and Bejan (2006)]. Heat transfer through a porous medium is a very common phenomenon. The natural tendency of fluid to expand when heated causes a density inversion to occur, if the heating is strong enough, a circulatory motion follows, termed convection. Convection in fluid layer is well-studied phenomenon and occurs in many natural settings: in the atmosphere, in the Earth's mantle and in many industrial applications including solidification and heating. Convection also occurs in a porous media. There are several applications of porous medium convection [Fowler (1997)]. The black smokers and white smokers on the ocean floor provide two interesting examples. A hydrothermal vent is a fissure in a planet's surface from which geothermally heated water issues. Hydrothermal vents are commonly found near volcanically active places, areas where tectonic plates are moving apart, ocean basins. Hydrothermal vents exist because the earth is both geologically active and has large amounts of water on its surface and within its crust. Under the sea, hydrothermal vents may form features called black smokers.These extraordinary edifices are vents that pour forth very hot water, massively contaminated with sulphides and other minerals, hence black color. Another example of porous medium convection is afforded by hot springs and geysers, such as those in Yellowstone National Park. A similar phenomenon can occur in domestic hot water systems, if they are incorrectly constructed.

Study of hydrodynamic and hydromagnetic stabilities has been an important research area since nineteenth century. Landau [Landau (1944)] proposed an equation to analyze hydrodynamic stability in 1944. The Landau equation has been derived for various cases by Drazin and Reid [Drazin and Reid (2004)] and the dependence of Landau constant for supercritical stability and subcritical stability has been discussed. Chandrasekhar in [Chandrasekhar (1961)] carried out extensive research work on hydrodynamic and hydromagnetic stability from 1950 to 1961. Fowler in [Fowler (1985)] developed a mathematical model for the convective flow in chimneys and predicted a criterion for the onset of convection and freckling. Worster developed and analyzed the governing equations for a mushy layer in the asymptotic limit of large solutal Rayleigh number [Worster (1991) and [Worster (1992)]. Riahi in [Riahi (1989)] carried out nonlinear stability analysis in a porous layer with permeable boundaries. The case of a continuous finite bandwidth of convection modes in a horizontal layer was analyzed by Riahi in [Riahi (1996)]. Bhatta et al. investigated linear marginal stability for magneto-convective flows in a mushy layer [Bhatta et al. (2010)]. Here we present the three dimensional model for a aquifer system in the second section. In the third section we present the solution technique and the fourth section details the derivation of the equation satisfied by the amplitude. Then we present marginal stability curve for this system and discuss numerical results of super-critical and sub-critical solutions for different values of space variables and time in the fifth section. The last section concludes the paper.

2. Governing System

We consider a permeable aquifer bounded above and below by impermeable boundaries and

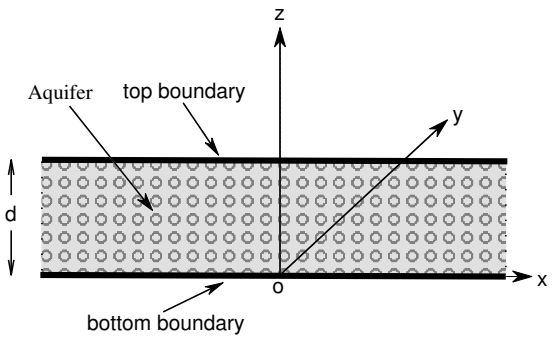

Fig. 1: A schematic diagram for the aquifer problem.

heated from below. Fowler in [Fowler (1997)] has presented a two-dimensional mathematical model for this case in detail. Here we follow the modeling idea described by him. We take the horizontal xy-plane as the bottom boundary of the aquifer and z-axis is vertical which is positive upward. The upper boundary of the aquifer is at a distance d parallel to the xy-plane. A schematic diagram for this problem is shown in figure 1.

Because convection is driven by thermally induced buoyancy, we assume that the density, ρ, of liquid at temperature, T, in the aquifer is given by

$$\rho = \rho_0 \left[1 - \alpha \left(T - T_0\right)\right], \tag{1}$$

where T_0 is a reference temperature, which is taken to be temperature at the top of the layer. Here α is coefficient of heat and ρ_0 is a reference density at T_0. Let the porosity of the rock be ϕ. The conservation of fluid mass in the rock yields

$$\frac{\partial}{\partial t}\left(\rho\phi\right) + \nabla \cdot \left(\rho \overrightarrow{u}\right) = 0, \tag{2}$$

where $\overrightarrow{u}$ is the fluid flux (equal to porosity times velocity). Darcy's law is

$$\overrightarrow{u} = -\frac{\mathscr{K}}{\mu}\left[\nabla p + \rho g \hat{k}\right], \tag{3}$$

where $\mathscr{K}$ is the permeability, μ is the liquid viscosity, p is the pressure, g is the gravity and $\hat{k}$ is unit vector vertically upward (z-direction). The energy equation is

$$\frac{\partial}{\partial t}\left[\left\{\rho\phi c_l + \rho_r\left(1-\phi\right)c_r\right\}T\right] + \nabla \cdot \left(\rho c_l \overrightarrow{u} T\right) = \nabla \cdot \left(k_T \nabla T\right), \tag{4}$$

where c_l, $c_r$are specific heats of liquid and rock, ρ_r is the density of rock, T is temperature and k_T is the average thermal conductivity. Here $k_T = \phi k_l + (1-\phi)k_r$ where k_l, k_r are the thermal conductivities of liquid and rock, respectively.

We prescribe boundary conditions

$$\begin{aligned} &T = T_0 + \triangle T, \qquad w = 0, \qquad at\ z = 0, \\ &T = T_0, \qquad\qquad\ w = 0, \qquad at\ z = d. \end{aligned} \tag{5}$$

Here, $\triangle T$ is the temperature difference, w is the vertical component of $\overrightarrow{u}$ and d is the layer depth. A typical value of α is $\sim 10^{-5}K^{-1}$, so that even if $\triangle T \sim 10^3 K$, as is likely for hydrothermal convection, we have the Boussinesq number

$$\mathscr{B} = \alpha \triangle T \ll 1. \tag{6}$$

It follows that where ρ appears algebraically in the equations, we approximate ρ as $\rho \approx \rho_0$, but $\mathscr{B}$ is retained whenever ρ appears as a derivative.

2.1. Nondimensionalization

We introduce nondimensionalized variables with asterisk and define those variables as follows

$$(x^*, y^*, z^*) = \left(\frac{x}{d}, \frac{y}{d}, \frac{z}{d}\right), \quad T^* = \frac{T - T_0}{\triangle T},$$
$$p^* = \frac{p - p_0 + \rho_0 g z}{[p]}, \quad \overrightarrow{u}^* = \frac{\overrightarrow{u}}{[u]}, \quad t^* = \frac{t}{[t]},$$

where

$$[u] = \frac{k_T}{\rho_0 c d}, \qquad [t] = \frac{d^2 \rho_m c}{k_T}, \qquad [p] = \frac{\mu k_T}{\rho_0 c \mathscr{K}},$$

with $\rho_m = \rho_0 \phi + \rho_r (1 - \phi)$. We take the specific heats c_l and c_r as equal to a constant c and take the thermal conductivity k_T as constant. Introduction of a nondimensional parameter, known as the Rayleigh number, given by

$$\mathscr{R} = \frac{\alpha \triangle T \rho_0^2 c g d \mathscr{K}}{\mu k_T} \tag{7}$$

and dropping the asterisk, nondimensional system becomes

$$-\mathscr{B}\left(\frac{\rho_0 \phi}{\rho_m}\right)\frac{\partial T}{\partial t} + \nabla \cdot [(1 - \mathscr{B}T)\,\overrightarrow{u}] = 0, \tag{8}$$
$$\overrightarrow{u} = -\nabla p + \mathscr{R} T \hat{k}, \tag{9}$$
$$\nabla^2 T = \left\{1 - \mathscr{B}\left(\frac{\rho_0 \phi}{\rho_m}\right) T\right\}\frac{\partial T}{\partial t} + (1 - \mathscr{B}T)\,\overrightarrow{u} \cdot (\nabla T), \tag{10}$$

with boundary conditions

$$T = 1, \quad w = 0, \qquad on \quad z = 0,$$
$$T = 0, \quad w = 0, \qquad on \quad z = 1. \tag{11}$$

3. Solution Procedure for the Aquifer System

Now we make use of Boussinesq approximation by letting $\mathscr{B} \to 0$ and $\frac{\rho_0 \phi}{\rho_m} < 1$. So, our aquifer system becomes

$$\nabla \cdot \overrightarrow{u} = 0, \tag{12}$$

$$\overrightarrow{u} = -\nabla p + \mathscr{R} T \hat{k}, \tag{13}$$

$$\nabla^2 T = \frac{\partial T}{\partial t} + \overrightarrow{u} \cdot (\nabla T), \tag{14}$$

with boundary conditions

$$\begin{aligned} T = 1, \quad w = 0, \qquad on \quad z = 0, \\ T = 0, \quad w = 0, \qquad on \quad z = 1. \end{aligned} \tag{15}$$

3.1. Basic State and Perturbed Systems

If we perturb the aquifer system given by (12) - (14) as follows

$$\begin{aligned} T(x,y,z) &= T_b(z) + \varepsilon \Theta(x,y,z), \\ \overrightarrow{u}(x,y,z) &= \overrightarrow{u}_b + \varepsilon \overrightarrow{U}(x,y,z), \\ p(x,y,z) &= p_b(z) + \varepsilon P(x,y,z), \end{aligned} \tag{16}$$

where $T_b, \overrightarrow{u}_b, p_b$ are solutions to the steady basic state system (system with no flow) and Θ, $\overrightarrow{U}$, P, are perturbed solutions, $\tau = \varepsilon t$ and ε is the perturbation parameter defined by $\varepsilon = \frac{\mathscr{R} - \mathscr{R}_c}{\mathscr{R}_1}$. Here $\mathscr{R}_c$ is the critical Rayleigh number and $\mathscr{R}_1$ is the contribution to $\mathscr{R}$ beyond the critical number.

3.1.1. Basic State System

The basic state is one with no motion. The basic state system is obtained by using the equations given by (16) in (12) - (14) and comparing the coefficients of ε^0 as follows

$$\overrightarrow{u}_b = \overrightarrow{0}, \tag{17}$$

$$\frac{\partial p_b}{\partial z} - \mathscr{R}_c T_b = 0, \tag{18}$$

$$\nabla^2 T_b = 0. \tag{19}$$

A reference pressure is supplied at the top boundary and we assume that $p_b = 0$ on $z = 1$. Boundary conditions on T_b are:

$$\begin{aligned} T_b = 1 \qquad on \ z = 0, \\ T_b = 0 \qquad on \ z = 1. \end{aligned}$$

The solutions of the basic state system can be obtained as

$$\overrightarrow{u}_b = \overrightarrow{0}, \tag{20}$$

$$T_b = 1 - z, \tag{21}$$

$$p_b = -\frac{\mathscr{R}_c}{2}(1-z)^2. \tag{22}$$

3.1.2. Perturbed System

The perturbed solutions satisfies the following system

$$\nabla \cdot \overrightarrow{U} = 0, \tag{23}$$

$$\overrightarrow{U} + \nabla P - (\mathscr{R}_c \Theta + \varepsilon \mathscr{R}_1 T_b)\hat{k} = \varepsilon \mathscr{R}_1 \Theta \hat{k}, \tag{24}$$

$$\nabla^2 \Theta - \frac{\partial \Theta}{\partial t} - W T_b' = -\overrightarrow{U} \cdot (\nabla \Theta), \tag{25}$$

with boundary conditions $\Theta = 0, W = 0$ on $\quad z = 0,\ 1$. Here W is the vertical component of $\overrightarrow{U}$ and T_b'=$\frac{dT_b}{dz}$. Now, we eliminate the pressure from the equation (24) by taking the double curl of that equation. Writing $\overrightarrow{U} = (U, V, W) = \nabla \times \nabla \times \left(U_P \overrightarrow{k}\right) + \nabla \times \left(U_T \overrightarrow{k}\right)$ (due to [Chandrasekhar (1961)] since $\nabla . \overrightarrow{U} = 0$), where U_P and U_T represent poloidal and toroidal components of $\overrightarrow{U}$ and using

$$\nabla \times \nabla \times \overrightarrow{f} = \left(\frac{\partial^2 f_3}{\partial x \partial z}, \frac{\partial^2 f_3}{\partial y \partial z}, -\frac{\partial^2 f_3}{\partial x^2} - \frac{\partial^2 f_3}{\partial y^2}\right)$$

and

$$\nabla \times \overrightarrow{f} = \left(\frac{\partial f_3}{\partial y}, -\frac{\partial f_3}{\partial x}, 0\right),$$

with $\overrightarrow{f} = (0, 0, f_3)$, we obtain

$$\overrightarrow{U} = (U, V, W) = \left(\frac{\partial^2 U_P}{\partial x \partial z} + \frac{\partial U_T}{\partial y}, \frac{\partial^2 U_P}{\partial y \partial z} - \frac{\partial U_T}{\partial x}, -\Delta_2 U_P\right),$$

where Δ_2 is 2-D Laplacian, i.e., $\Delta_2 = \frac{\partial^2}{\partial x^2} + \frac{\partial^2}{\partial y^2}$.

Using the continuity equation $\frac{\partial U}{\partial x} + \frac{\partial V}{\partial y} + \frac{\partial W}{\partial z} = 0$, we obtain the third component of $\nabla \times \nabla \times \overrightarrow{U}$ as

$$\begin{aligned}
&\frac{\partial^2 U}{\partial x \partial z} + \frac{\partial^2 V}{\partial y \partial z} - \frac{\partial^2 W}{\partial x^2} - \frac{\partial^2 W}{\partial y^2} \\
&= -\frac{\partial^2 W}{\partial z^2} - \frac{\partial^2 W}{\partial x^2} - \frac{\partial^2 W}{\partial y^2} \\
&= -\nabla^2 W = \nabla^2 (\Delta_2 U_P).
\end{aligned}$$

Similarly, for the third component of $\nabla \times \nabla \times (\mathscr{R}\Theta \overrightarrow{k})$, we have

$$-\mathscr{R}\left[\frac{\partial^2\Theta}{\partial x^2}+\frac{\partial^2\Theta}{\partial y^2}\right]=-\mathscr{R}(\Delta_2\Theta).$$

These allow us to write equation (24) as

$$\nabla^2 W-\mathscr{R}_c\left(\Delta_2\Theta\right)=\varepsilon\mathscr{R}_1\left(\Delta_2\theta\right). \tag{26}$$

Thus, the three dimensional perturbed system becomes

$$\begin{aligned}
&\nabla^2\left(\Delta_2 U_P\right)+\mathscr{R}_c\left(\Delta_2\Theta\right)=-\varepsilon\mathscr{R}_1\left(\Delta_2\Theta\right),\\
&\nabla^2\Theta+\left(\Delta_2 U_P\right)T_b'=\varepsilon\left[\frac{\partial\Theta}{\partial\tau}+C\left(\frac{\partial^2 U_P}{\partial x\partial z}+\frac{\partial U_T}{\partial y}\right)\frac{\partial\Theta}{\partial x}\right.\\
&\qquad\left.+\left(\frac{\partial^2 U_P}{\partial y\partial z}-\frac{\partial U_T}{\partial x}\right)\frac{\partial\Theta}{\partial y}-\left(\Delta_2 U_P\right)\frac{\partial\Theta}{\partial z}\right],\\
&\Delta_2 U_T=0,
\end{aligned} \tag{27}$$

with boundary conditions $\Theta=0=U_P=U_T$ on $z=0,\ 1$.

For two dimensional case, we have

$$\nabla^2\left(\Delta_2 U_P\right)+\mathscr{R}_c\left(\Delta_2\Theta\right)=-\varepsilon\mathscr{R}_1\left(\Delta_2\Theta\right), \tag{28}$$

$$\nabla^2\Theta+\left(\Delta_2 U_P\right)T_b'=\varepsilon\left[\frac{\partial\Theta}{\partial\tau}+\frac{\partial^2 U_P}{\partial x\partial z}\frac{\partial\Theta}{\partial x}-\left(\Delta_2 U_P\right)\frac{\partial\Theta}{\partial z}\right], \tag{29}$$

and the boundary conditions are $\Theta=0=U_P$ on $z=0,\ 1$.

3.2. 2-D Linear and First-order Systems

Considering

$$\begin{aligned}
\Theta&=\Theta_0+\varepsilon\Theta_1+\varepsilon^2\Theta_2+\cdots,\\
U_P&=U_{P_0}+\varepsilon U_{P_1}+\varepsilon^2 U_{P_2}+\cdots,
\end{aligned}$$

where the number in the sub-index represents the order of the perturbed system, the linear system can be expressed from (28) as

$$\begin{aligned}
&\nabla^2\left(\Delta_2 U_{P_0}\right)+\mathscr{R}_c\left(\Delta_2\Theta_0\right)=0,\\
&\nabla^2\Theta_0+\left(\Delta_2 U_{P_0}\right)T_b'=0,
\end{aligned}$$

or

$$\nabla^2 W_0-\mathscr{R}_c\left(\Delta_2\Theta_0\right)=0, \tag{30}$$

$$\nabla^2\Theta_0-T_b' W_0=0, \tag{31}$$

and the first-order systems can be written (29) as

$$\nabla^2 W_1 - \mathscr{R}_c \left(\Delta_2 \Theta_1\right) = \mathscr{R}_1 \left(\Delta_2 \Theta_0\right), \tag{32}$$

$$\nabla^2 \Theta_1 - T_b' W_1 = \frac{\partial \Theta_0}{\partial \tau} + \frac{\partial^2 U_{P_0}}{\partial x \partial z} \frac{\partial \Theta_0}{\partial x} - \left(\Delta_2 U_{P_0}\right) \frac{\partial \Theta_0}{\partial z}, \tag{33}$$

respectively. If we express the linear solutions in the form $f_0(x,z,\tau) = A(\tau)\,\tilde{f}_0(z)\,\eta(x)$, where A represents amplitude and $\eta(x) = Re\left\{e^{ikx}\right\}$ with k as the wavenumber. Then the linear PDE system given by (30) and (31) can be obtained as a linear ODE system

$$\left(D^2 - k^2\right) \widetilde{W}_0 + k^2 \mathscr{R}_c \widetilde{\Theta}_0 = 0, \tag{34}$$

$$\left(D^2 - k^2\right) \widetilde{\Theta}_0 + k^2 \widetilde{W}_0 = 0, \tag{35}$$

with $D = \frac{d}{dz}$.

4. Derivation of Amplitude Equation

Now we derive the equation satisfied by the amplitude $A(\tau)$ by introducing the concept of adjoint system. We denote dependent variables for the adjoint system as w_a and θ_a. To obtain the adjoint system, we multiply the equations given by linear system, namely, (30) and (31) by w_a and θ_a respectively, add them and integrate and then take the limit as follows

$$\lim_{L\to\infty} \frac{1}{2L} \int_0^1 \int_{-L}^{L} \left[w_a \left(\nabla^2 W_0\right) - \mathscr{R}_c w_a \left(\Delta_2 \Theta_0\right) + \theta_a \left(\nabla^2 \Theta_0\right) - \theta_a T_b' W_0\right] dx dz = 0. \tag{36}$$

Here, L denotes the length in x-direction. The boundary conditions satisfied by adjoint solutions are $\theta_a = 0 = w_a$ on $\quad z = 0,\ 1$. After carrying out integration by parts and taking the limit, we obtain the adjoint system as

$$\nabla^2 w_a - T_b' \theta_a = 0,$$
$$\nabla^2 \theta_a - \mathscr{R}_c \left(\Delta_2 w_a\right) = 0.$$

To derive the equation satisfied by the amplitude, we use the first-order system. We multiply equations (32) and (33) by w_a and θ_a, respectively, add the result, integrate, and take the limit. The left hand side of this operation becomes

$$LHS = \lim_{L\to\infty} \frac{1}{2L} \int_0^1 \int_{-L}^{L} \left[w_a \left\{\nabla^2 W_1 + \mathscr{R}_c \left(\Delta_2 \Theta_1\right)\right\} + \theta_a \left\{\nabla^2 \Theta_1 - T_b' W_1\right\}\right] dx\, dz. \tag{37}$$

The right hand side is given by

$$RHS = \lim_{L\to\infty} \frac{1}{2L} \int_0^{\delta} \int_{-L}^{L} \int_{-L}^{L} \left[w_a \mathscr{R}_1 \left(\Delta_2 \Theta_0\right) + \theta_a \left\{\frac{\partial \Theta_0}{\partial \tau} + \frac{\partial^2 U_{P_0}}{\partial x \partial z} \frac{\partial \Theta_0}{\partial x} - \left(\triangle_2 u_{P_0}\right) \frac{\partial \theta_0}{\partial z}\right\}\right] dx\, dz. \tag{38}$$

Integration by parts and use of boundary conditions simplify left hand side as

$$LHS = \lim_{L\to\infty} \frac{1}{2L} \int_0^1 \int_{-L}^{L} \left[W_1 \left\{ \nabla^2 w_a - T_b' \theta_a \right\} + \Theta_1 \left\{ \nabla^2 \theta_a - \mathscr{R}_c \left(\Delta_2 w_a \right) \right\} \right] dx\, dz,$$

which is zero because of the adjoint system. Now we simplify right hand side by writing as

$$RHS = I_1 + I_2 + I_3 + I_4, \tag{39}$$

where

$$\begin{aligned} I_1 &= \lim_{L\to\infty} \frac{1}{2L} \int_0^1 \int_{-L}^{L} w_a \mathscr{R}_1 \left(\Delta_2 \Theta_0 \right) dx\, dz, \\ I_2 &= \lim_{L\to\infty} \frac{1}{2L} \int_0^1 \int_{-L}^{L} \theta_a \frac{\partial \Theta_0}{\partial \tau} dx\, dz, \\ I_3 &= \lim_{L\to\infty} \frac{1}{2L} \int_0^1 \int_{-L}^{L} \theta_a \frac{\partial^2 U_{P_0}}{\partial x \partial z} \frac{\partial \Theta_0}{\partial x} dx\, dz, \\ I_4 &= \lim_{L\to\infty} \frac{1}{2L} \int_0^1 \int_{-L}^{L} \left\{ -\theta_a \left(\triangle_2 U_{P_0} \right) \frac{\partial \Theta_0}{\partial z} \right\} dx\, dz. \end{aligned} \tag{40}$$

We assume that the linear and adjoint solutions take the following form

$$f(x, z, \tau) = A(\tau) \widetilde{f}(z) \eta(x). \tag{41}$$

Here, A represents the amplitude, $\eta(x) = Re\left[e^{ikx}\right]$, and k is the wavenumber. Now we can simplify the integrals appearing in (40) as follow

$$\begin{aligned} I_1 &= -k^2 \mathscr{R}_1 A^2 \left\{ \int_0^1 \widetilde{w}_a \widetilde{\Theta}_0 dz \right\} \left(I_{\eta^{(2)}} \right), \\ I_2 &= A \frac{dA}{d\tau} \left\{ \int_0^1 \widetilde{\theta}_a \widetilde{\Theta}_0 dz \right\} \left(I_{\eta^{(2)}} \right), \\ I_3 &= A^3 C \left\{ \int_0^1 \widetilde{\theta}_a \widetilde{\Theta}_0 \left(D\widetilde{U}_{P_0} \right) dz \right\} \left(I_{\eta^{(12)}} \right), \\ I_4 &= -k^2 A^3 C \left\{ \int_0^1 \widetilde{\theta}_a \widetilde{U}_{P_0} \left(D\widetilde{\Theta}_0 \right) dz \right\} \left(I_{\eta^{(3)}} \right), \end{aligned} \tag{42}$$

where $D = \frac{d}{dz}$ and $I_{\eta^{(2)}}$, $I_{\eta^{(12)}}$, $I_{\eta^{(3)}}$ are given by

$$\begin{aligned} I_{\eta^{(2)}} &= \lim_{L\to\infty} \frac{1}{2L} \int_{-L}^{L} \eta^2 dx, \\ I_{\eta^{(12)}} &= \lim_{L\to\infty} \frac{1}{2L} \int_{-L}^{L} \eta \left(\frac{\partial \eta}{\partial x} \right)^2 dx, \\ I_{\eta^{(3)}} &= \lim_{L\to\infty} \frac{1}{2L} \int_{-L}^{L} \eta^3 dx. \end{aligned} \tag{43}$$

Carrying out the integrations and taking the limits, we obtain an equation satisfied by the amplitude as

$$a_1 \frac{dA}{d\tau} = a_2 A, \tag{44}$$

where $a_1 = \int_0^1 \widetilde{\theta}_a \widetilde{\Theta}_0 dz$ and $a_2 = k^2 \mathscr{R}_1 \int_0^1 \widetilde{w}_a \widetilde{\Theta}_0 dz$. Solution of the equation (44) is obtained as $A(\tau) = A_0 e^{a\tau}$. Here $A_0 = A(0)$ the initial value of A and $a = \frac{a_2}{a_1}$.

5. Results and Discussion

Here we present results obtained using numerical procedures. First we obtain the critical Rayleigh number and critical wavenumber. These are obtained solving an ODE the system which is obtained from the PDE system (30) and (31) using (41). The critical pair $(k_c, \mathscr{R}_c)$ is found to be (3.1415926, 39.478418245) using fourth-order Runge-Kutta Method in combination of shooting method [Cheney and Kincaid (2008)]. Marginal stability curve is shown in Figure (2).

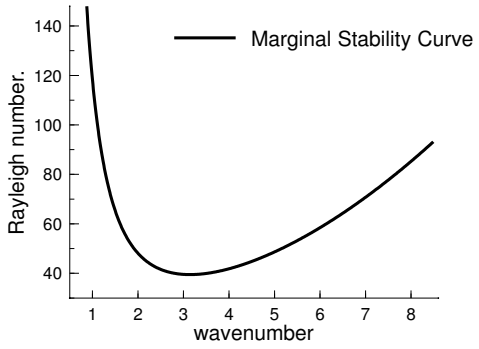

Fig. 2: Marginal stability curve.

Linear temperature which is a solution of the system given by (34)-(35) is displayed in Figure (3). It is observed temperature is highest at the the center of the aquifer and decreases to zero at the bottom and top of the aquifer. Also it is found from numerical results that vertical velocity which is related to poloidal component follows a similar pattern, i.e., vertical velocity component has more influence at the center and zero effect at the top and bottom.

Solution of the amplitude equation (44) is presented in Figure (4). Since $\mathscr{R} = \mathscr{R}_c + \varepsilon \mathscr{R}_1$ and $\varepsilon > 0$, we have $\mathscr{R}_1 > 0$ for super-critical case and $\mathscr{R}_1 < 0$ for sub-critical case. For our numerical calculations we use $\varepsilon = 0.001$. Solid line represents the solutions of amplitude equation for the sub-critical case and dashed line denotes the solutions of amplitude equation for the super-critical case. It is seen that amplitude grows (unstable) for super-critical case and decays (stable) for sub-critical case. Asymptotic values are ∞ for super-critical case and 0 for sub-critical case.

Figures (5)-(12) present the solution for temperature variable which satisfies the system (30)-(31). Comparison of solutions for different values of x for the sub-critical case are shown in

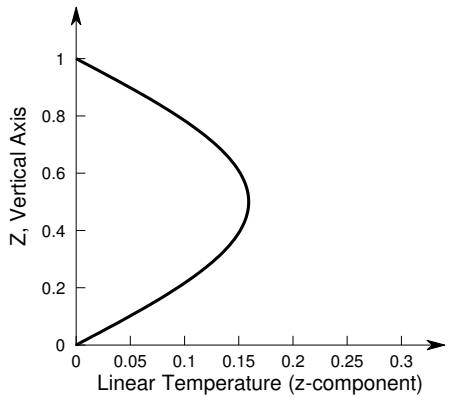

Fig. 3: Linear temperature $\tilde{\Theta}_0$, solution of the system (34) and (35).

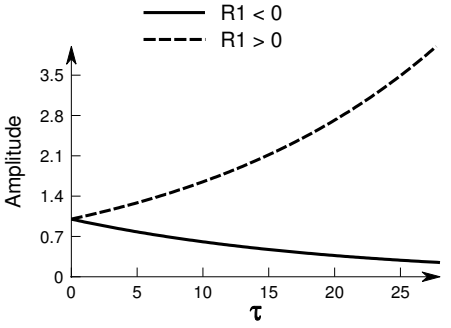

Fig. 4: Amplitude, solution of the equation (44).

Figure (5) for a particular time $\tau = 4$ at $x = 0.0, 0.4, 0.8$. It is noticed from numerical results that temperature is highest at $x = 0.0$. It decreases as x increases from 0.0 to 0.5. From $x = 0.5$ to $x = 1.0$, temperature changes its sign and becomes lowest at $x = 1.0$, then it starts increasing again.

Figure (6) presents comparison of solutions for the sub-critical case at three different values of z, namely, $z = 0.2, 0.5, 0.7$. It is observed that the solution is periodic with respect to x and one period is $(-1.0, 1.0)$.

Super-critical solutions at $x = 0.0$ are shown in Figure (7) for different times. It is observed that solutions have higher amplitudes for higher times. Figure (8) displays sub-critical solutions at $x = 0.0$ for different times. We see that solutions decay as times increase.

Figure (9) presents super-critical solutions at a particular height $z = 0.5$ for various times. It is noticed that amplitudes of the solutions grow for higher times. Sub-critical solutions at $z = 0.5$ for different times are shown in Figure (10). The solution is a decreasing function of time. It is also observed that solutions for both super-critical and sub-critical cases are periodic with respect to x with the same period.

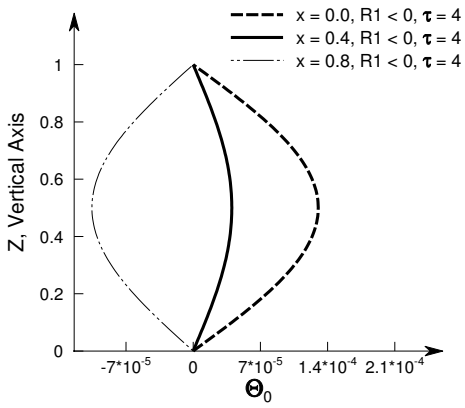

Fig. 5: Comparison of sub-critical temperatures ($R_1 < 0$) for different values of x at $\tau = 4$.

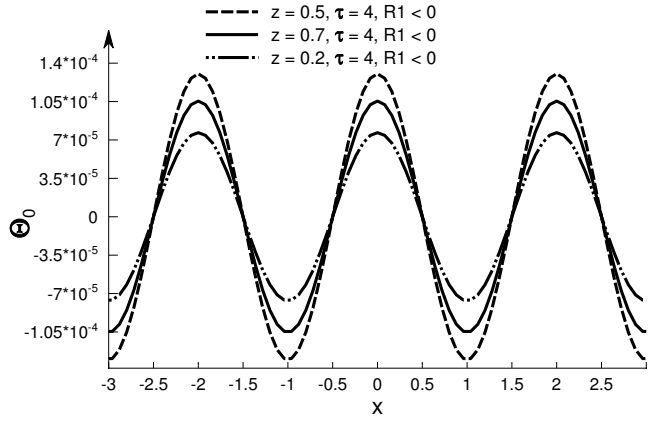

Fig. 6: Comparison of sub-critical temperatures ($R_1 < 0$) for different values of z at $\tau = 4$.

Figures (11) and (12) compare numerical solutions for temperature for $\mathscr{R}_1 > 0$ and $\mathscr{R}_1 < 0$. Super-critical and sub-critical solutions for a particular time $\tau = 4$ at $x = 0.0$ are shown in Figure (11).

Figure (12) compares the super-critical and sub-critical solutions for that time at a height $z = 0.5$. Numerical results suggest that sub-critical solution for temperature is stable and super-critical solution for temperature is unstable. Similar conclusion can be made for the velocity component from our numerical results.

6. Conclusion

We compute the solutions for temperature due to hydro-thermal convection in an aquifer system which is heated from below. Marginal stability curve is obtained by using Runge-Kutta method in combination of shooting method. Equation satisfied by the amplitude is derived with the help of the adjoint system. Numerical procedure estimates the critical wavenumber and critical

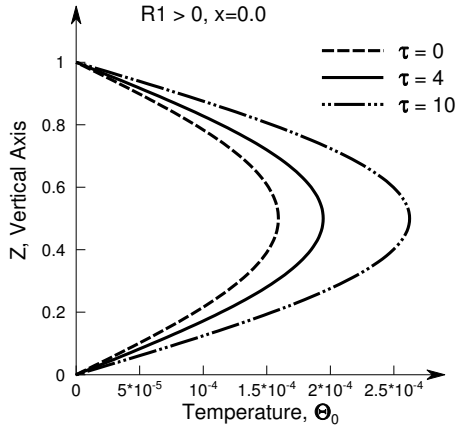

Fig. 7: Super-critical temperatures at $x = 0.0$ for $\mathscr{R}_1 > 0$ at different times $\tau = 0,\ 4,\ 10$.

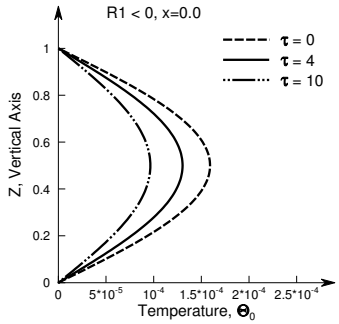

Fig. 8: Sub-critical temperatures at $x = 0.0$, $\mathscr{R}_1 < 0$ at different times $\tau = 0,\ 4,\ 10$.

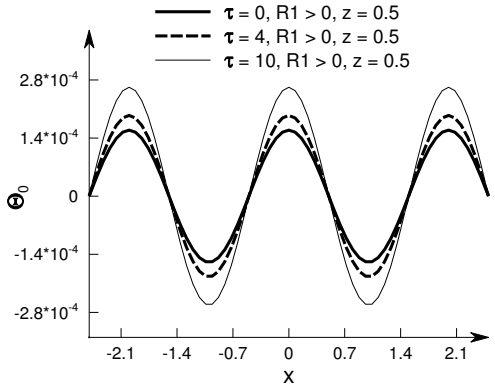

Fig. 9: Super-critical temperatures at $z = 0.5$, $\mathscr{R}_1 > 0$ at different times $\tau = 0,\ 4,\ 10$.

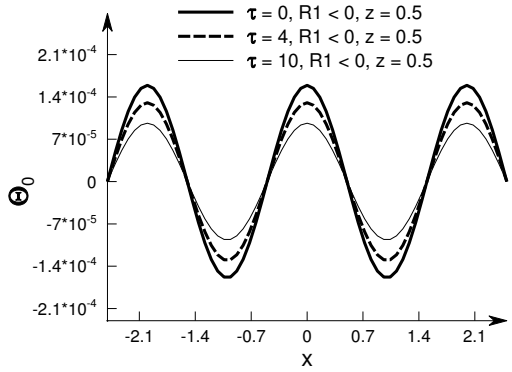

Fig. 10: Sub-critical temperatures at $z = 0.5$, $\mathscr{R}_1 < 0$ at different times $\tau = 0,\ 4,\ 10$.

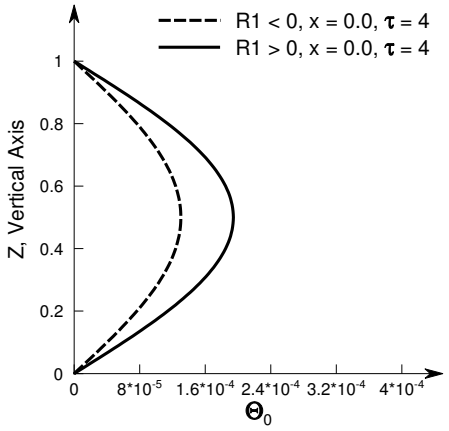

Fig. 11: Comparison of super-critical and sub-critical temperatures as functions of z at $\tau = 4$.

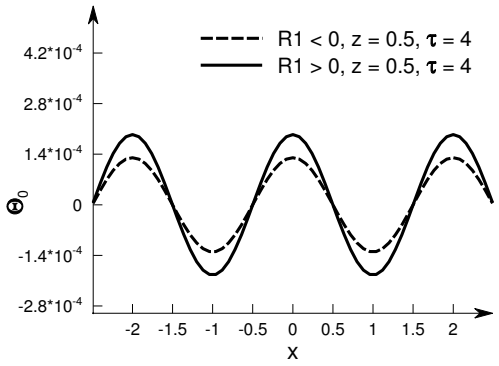

Fig. 12: Comparison of super-critical and sub-critical temperatures as functions of x at $\tau = 4$.

Rayleigh number as 3.1415926 and 39.478418245 respectively. Solutions of the ODE system are functions of the space variable z only. It is observed that temperature starts increasing and reaches maximum at the middle of the layer and then starts decreasing reaching zero at the top

boundary. This indicates that the most of the activity occurs along the center of the aquifer. Solutions of the system are periodic with respect to the space variable x and the period is of length 2 with one period (-1, 1). The amplitude function is increasing for super-critical case and decreasing for sub-critical case. As time increases, the solutions arising from super-critical case tend to increase, but for sub-critical case, solutions decrease. These imply that the super-critical system is unstable and sub-critical system is stable which is supported by the numerical results.

Acknowledgment

Author would like to thank the reviewers for their constructive comments and suggestion to improve the manuscript.

References

Nield, D. A. and Bejan, A. (2006). Convection in a Porous Media, Springer, NY.

Fowler, A. C. (1997). Mathematical Models in the Applied Sciences, Cambridge University Press, Cambridge.

Landau L. D. (1944). On the problem of turbulence, C.R. Acad. Sci. U.R.S.S **44**, pp. 311-314

Drazin, P. G. and Reid, W. H. (2004). Hydrodynamic Stability, Second Edition, Cambridge University Press, Cambridge.

Chandrasekhar, S. (1961). Hydrodynamic and Hydromagnetic Stability, Dover Publication, NY.

Fowler, A. C. (1985). The formation of freckles in binary alloys, IMA J. Appl. Maths., **35**, pp. 159-174.

Worster, M. G. (1991). Natural convection in a mushy layer, J. Fluid Mech., **224**, pp. 335-359.

Worster, M. G. (1992). Instabilities of the liquid and mushy regions during solidification of alloys, J. Fluid Mech., **237**, pp. 649-669.

Riahi, D. N. (1989). Nonlinear convection in a porous layer with permeable boundaries, Int. J. Non-Linear Mech., **24**, pp. 459-463.

Riahi, D. N. (1996). Modal package convection in a porous layer with boundary imperfections, J. Fluid Mech., **318**, pp. 107-128.

Bhatta, D., Muddamallappa, M. S. and Riahi, D. N. (2010). On perturbation and marginal stability analysis of magneto-convection in active mushy layer, Transport in Porous Media, **82**, pp. 385-399.

Cheney, W. and Kincaid, D. (2008). Numerical Mathematics and Computing, Thomson Brooks/Cole, 6th edition.